Netherlands
organization for
applied scientific
research

TNO-report

TNO Physics and Electronics
Laboratory

P.O. Box 96864
2509 JG The Hague
Oude Waalsdorperweg 63
The Hague, The Netherlands

Fax +31 70 328 09 61
Phone +31 70 326 42 21

report no. FEL-90-A352

copy no. 9

title

A high repetition rate LIDAR

author:

Ir. G.J. Kunz

date :

April 1991

Original contains color plates: All DTIC reproductions will be in black and white

classification

title	: unclassified
abstract	: unclassified
report text	: unclassified

no. of copies	: 35
no. of pages	: 41 (excl. RDP & distribution list)
appendices	: -

All information which is classified according to Dutch regulations shall be treated by the recipient in the same way as classified information of corresponding value in his own country. No part of this information will be disclosed to any party.

report no. : FEL-90-A352
title : A high repetition rate LIDAR

author(s) : Ir. G.J. Kunz
Institute : TNO Physics and Electronics Laboratory

date : April 1991
NDRO no. : A84KL122
no. in pow '90 : 715.1

Research supervised by: Drs. C.W. Lamberts
Research carried out by: Ir. G.J. Kunz

ABSTRACT (UNCLASSIFIED)

Using optical radar (LIDAR) techniques, properties of the atmosphere can be determined by remote sensing. Examples are, e.g., the horizontal visibility or the extinction coefficient, the vertical extinction or visibility profile and the cloud base altitude. Because the time scales in the atmosphere are much shorter than the maximum sample rate of the lidar available at the start of this project, a need existed of a system with a repetition rate of at least 10 pulses per second. With such a system it is possible to measure the dynamics of the atmosphere on a sub-second time scale and to map smoke and dust clouds. This report describes the properties of such a system, designed and developed at the Physics and Electronics Laboratory TNO. Some typical examples of results obtained with this system are presented. This is the final report of the work performed under assignment A84KL122.

rapport no.	:	FEL-90-A352
titel	:	Een LIDAR met een hoge herhalingsfrequentie
auteur(s)	:	Ir. G.J. Kunz
instituut	:	Fysisch en Elektronisch Laboratorium TNO
datum	:	april 1991
hdo-opdr.no.	:	A84KL122
no. in iwp '90	:	715.1
Onderzoek uitgevoerd o.l.v.	:	Drs. C.W. Lamberts
Onderzoek uitgevoerd door	:	Ir. G.J. Kunz

SAMENVATTING (ONGERUBRICEERD)

Met behulp van optische radar (LIDAR) technieken kunnen eigenschappen van de atmosfeer op afstand bepaald worden. In horizontale zin is dat bijvoorbeeld het zicht of de extinctie coefficient en in vertikale zin het extinctie- of het zicht-profiel en de wolkenbasishoogte. Daar de tijdschalen in de atmosfeer veel korter zijn dan gemeten kon worden met de lidar-apparatuur die ons bij het begin van dit project ter beschikking stond, was er behoefte aan een lidarsysteem met een herhalingsfrequentie van tenminste 10 Hz. Hiermede is het dan mogelijk dynamische verschijnselen van de atmosfeer op een tijdschaal van onderdelen van een seconde vast te leggen. Voorbeelden zijn het dynamisch gedrag van de atmosfeer en de omvang en ontwikkeling van rook- en stofwolken. Dit rapport beschrijft de eigenschappen van een dergelijk, op het Fysisch en Elektronisch Laboratorium TNO gerealiseerd, lidar-systeem. Enige typische voorbeelden van verkregen meetresultaten worden gepresenteerd. Dit is het eind-rapport van de werkzaamheden die zijn uitgevoerd in het kader van opdracht A84KL122.

1 INTRODUCTION

Lidar (LIght Detection And Ranging) is the optical equivalent of radar, working in the spectral range from about 200 nm to about 10 μm. In general lidars are applied for the remote sensing of some inherent atmospheric properties or for the detection of aerosol or gaseous species. Furthermore atmospheric dynamics can be studied if the repetition rate is high enough. Examples of lidar-measured quantities are:

- extinction and backscatter coefficient
- visibility
- cloud base altitude
- vertical extinction or backscatter profile
- concentration of gaseous species (ozone, water vapour, methane, etc)
- wind speed and wind direction
- temperature
- water depth
- ...

In general the range of a lidar system is of the order of some kilometers. The most powerful system known is Japanese, (Sasano, 1982) with a maximum range of about 30 km. When used as a range finder for solid targets, the maximum range is much larger. Rangefinders are limited by the transmission of the atmosphere, the target reflection and the sensitivity of the system.

Lidar systems developed and employed at the TNO Physics and Electronics Laboratory thus far (7 in total) had a relatively low repetition rate (less than one Hertz, e.g., Lamberts, 1974 and Kunz, 1978) and were well suited for their tasks. They were used in both national and international experiments over land (Kunz, 1982; 1984). Furthermore they were used over the North Atlantic aboard a ship (De Leeuw, 1984 .. 1989). For a number of purposes, it is desirable, or even required, to use a lidar system with a repetition rate of 10 or 20 Hz. With a high repetition rate lidar the atmosphere can more or less be frozen by a fast scan in one or more planes (Range to Height Indicator or RHI and/or Plane Position Indicator or PPI). This provides the possibility to map plumes and clouds over large areas. Furthermore the mobility and size of spatial inhomogeneities can be monitored by repetitive measurements along a plane or a volume. This

means that also the wind speed can indirectly be measured by following eddies trough the aerosol variations. Finally the performance of alternative lidar inversion techniques for measuring the vertical structure can be tested without the need of additional information (Kunz, 1988).

In this report we describe the realisation of a lidar system with a maximum repetition rate of about 13 Hz. It is refered to as 'SMAL', an acronym for Scanning Miniature Automatic Lidar. Some typical results as well as some features of the system will be presented in this report.

2 DESCRIPTION OF THE SYSTEM

Roughly, a lidar system can be subdivided into the transmitter, the receiver, the registration system and the control unit. In addition, SMAL has been mounted on a platform that is adjustable in both elevation and azimuth, to allow for measurements in any desired direction. The realisation and the properties of these parts in SMAL are discussed below in separate sections. The complete lidar system is shown in Figure 2.1. The main unit is the large box with the logo 'LIDAR'. An auxiliary lidar, which can be pointed in a different direction, has been mounted on top. The large (black) apertures are the optical receiver channels and the small holes in between those two are the output apertures for the laser beam. A television camera for surveillance purposes has been mounted behind the third optical channel in the main unit.

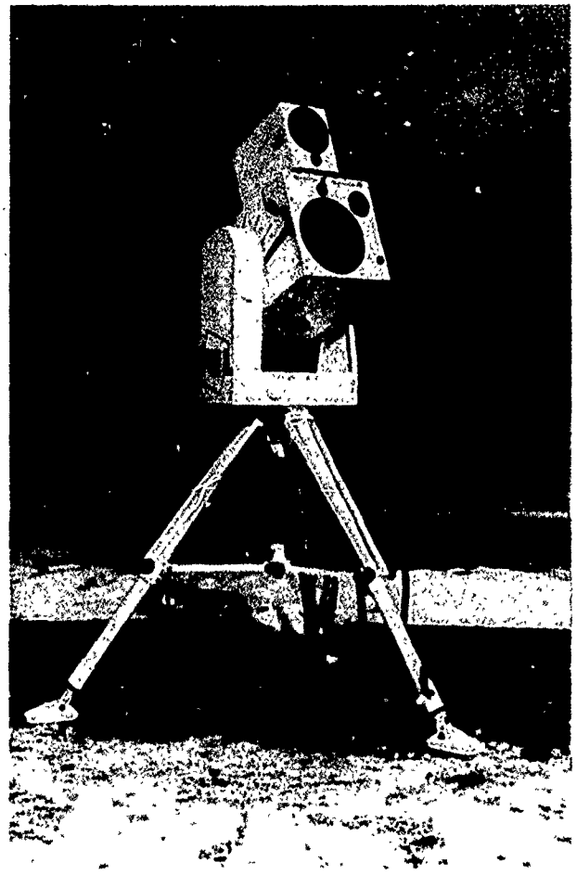

Fig. 2.1: The 'SMAL' dual mode lidar system. The system is mounted on a platform that is adjustable in azimuth and elevation.

The transmitter is a flash tube pumped Nd:YAG laser. The laser was developed in-house for easy fitting in the lidar and for easy service. The laser rod and the flash tube are mounted in a common housing which is flushed with distilled water (and a few percent ethanol) to drain the superfluous heat via a closed water circuit. Around the laser rod and the lamp a gold plated brass reflector has been constructed to improve the pump efficiency of the laser. The electrical connections of the flashtube are left outside the housing to keep them dry. A free optical path for the laser beam is obtained by additional holes in the housing which are sealed with O-rings around the laser rod.

Finally a spark plug has been mounted in the solid housing (in fact a high voltage feed-through with a tungsten wire which touches only the lamp) for the ignition of the simmer mode.

The resonator of the laser has a length of 40 cm. The back mirror has a reflectivity of 99,9 %; the front mirror has a reflectivity of 50 %. Both mirrors are coated for 1064 nm. An aluminum profile gives the resonator sufficient mechanical rigidity against bending. A zerodur rod, embedded in araldite, has been mounted in the center of the aluminum profile for stabilisation of the resonator length against temperature variations. The output obtained in this way is of the order of 100 mJ, in the normal laser mode. For lidar work however, the laser must be operated in the single pulse mode. This was achieved with a passive Q-switch of a thin nickel complex layer of bis(4-dimethylaminodithiobenzil) nickel (BDN) from Eastman Kodak, dissolved in dichloromethane. This way of Q-switching is both simple and reliable compared with rotating prisms or Pockels cells that are commonly used. The location of the cuvette with the bleachable dye in the resonator appeared not critical; for mechanical reasons it was decided to place it close to the front mirror. The available output of the laser in the Q-switched mode decreased however to about 20 mJ, independent of the concentration BDN or the pump energy. A maximum repetition rate of 13 Hz was obtained, limited in this set-up by the power supply. The properties of the laser transmitter are summarized in Table 2.1.

Table 2.1: Properties of the laser transmitter for the lidar.

Laser material	Nd:YAG; 0.9 %; Union Carbide
Laser wavelength	1064 nm
Rod dimensions	l= 50 mm; d= 5 mm
Flashtube	EG&G, FXQ 274-2
Q-switching dye	Kodak 14015 (BDN)
Solvent	dichloromethane
Dye thickness	1 mm
Energy per pulse	20 mJ
Pulse width	20 ns
Divergence	2.2 mrad
Pump capacitor	60 µF
Series inductance	20 µH; toroid
Repetition rate	15 Hz max.
Cooling system	NESLAB CFT-25
Coolant	10 % ethanol in distilled water
Flow	about 2 liters per minute
Deionisor	Permutit CD-250
Power consumption	1 kW overall.

The electric circuit, consisting of a capacitor of 60 μF and an inductance of the order of 20 mH, can be charged with a voltage between 600 and 1000 V. The inductance was realized as a toroid because other constructions induced very large currents in the housing as well as in the cables, due to the very strong external magnetic field. It can be shown, from the optical output and the electrical input, that the overall efficiency is of the order of 0.3 %. The laser unit is shown in Figure 2.2.

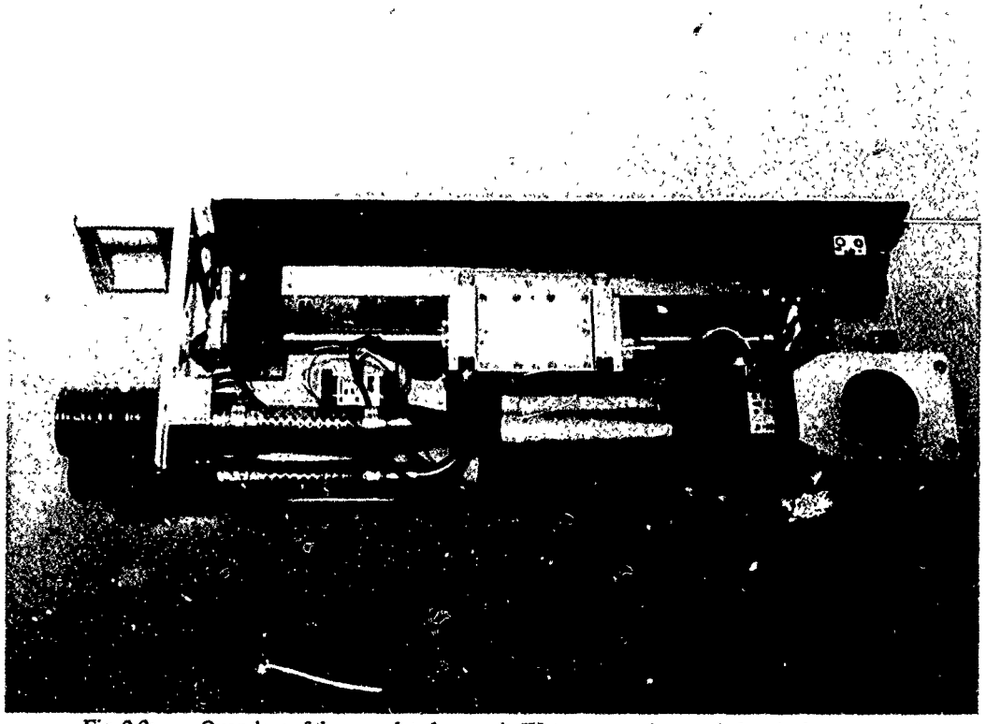

Fig. 2.2: Overview of the complete laser unit. Water connections and electrical power supply are at the front left end of the box. The other electrical connections, at the back end of the box, are plugs fitting into connections in the lidar. Laser head, toroid, cuvette and mirrors are visible.

Receivers for the lidar consist of a collimating telescope and an avalanche photodetector in the focal plane, to convert the optical radiation into an electrical signal. Because the system was designed with two simultaneous measuring channels, two receivers were installed. The main receiver has a diameter of 8 inch and the auxiliary channel has a diameter of 5 inch. The reverse

voltage for the detectors are temperature controlled to keep the gain at a fixed value. Optical interference filters and diaphragms are placed in the optical path to reduce the background-induced noise and the field of view. Amplifiers for the lidar are constructed such that the (daylight) background induced noise can be made visible. Other properties of the receiver are summarized in Table 2.2.

Table 2.2: Specifications of the optical receivers.

Main telescope	Celestron 2000
Effective area	2.19 E-8 km^2
Auxiliary telescope	Celestron 750
Effective area	9.35 E-9 km^2
Filter	3 cavities; T = 67 %
Detector	RCA C30916E
Sensitivity	12 A/W
Amplifier	120 kV/W
Rise time	25 ns
Dark noise	1.5 mV
Max. output signal	6 V into 50 Ω

Both the amplification factor and the electrical bandwidth of the receivers can be remotely set. In this way very strong signals, e.g., from hard targets, can be attenuated. Weak signals originating from extended targets and at large distances can be processed with a reduced bandwidth to suppress the noise.

The large dynamic range of lidar signals, within a fraction of a second, make their registration extra difficult. One of the solutions for this problem is to apply a logarithmic amplifier. These units generally have a logarithmic transfer for large signals and a constant transfer for small signals. In this way the dynamic range of the lidar signals can be electrically diminished before digitizing the stronger part of the signal while the weaker part is unaffected. A report on this subject has recently been published (Kunz, 1990).

Mechanical set up. The lidar is mounted on a platform which can be scanned in both azimuth and elevation angle. The platform in turn is mounted on a tripod which is adjustable in height. In this way the system can measure over 356 degrees in azimuthal direction and from -15 degrees to +95 degrees in vertical direction. Feedback of both the position and the speed provides a direction accuracy of less than 1 mrad in azimuth and less than 0.5 mrad in elevation. The minimum and

maximum speed in both directions is respectively 0.4 and 72 degrees per second. The platform electronics can be controlled by computer via the IEEE 488 bus. The settings can be stored in the memory of the platform and, once programmed, it can perform the selected motion without further computer or manual assistance. The position can be read by position sensors. This information is necessary for processing of the signals.

Electronics for recording and processing

Apart from the electronics for controlling the laser and the detectors, a transient recorder and a computer with a sufficient large storage capacity are required. For example, when the system is running at 8 Hz, 1 MByte of data or more is generated each minute depending on the record length. Furthermore a television monitor, a printer and a simple A/D converter are part of the hardware. A specification of the additional equipment is summarized in Table 2.3. With the available equipment it is possible to record waveforms of 1024 samples with a repetition rate of about 16 Hz.

Table 2.3: Other equipment necessary to run the lidar

Transient Recorder	Tektronix 7612D
Monitor	Tektronix 604
Pre-Processing	1. Analog Modules LA-90-P 2. Optec OS-LA-5-20
Computer	HP Vectra; 80286
Display	Barco CD 233
Graphics adapter	Tecmar Graphics Master
IEEE 488 interface	Tecmar PC Master
AD/DA converter	Tecmar Labtender
Video camera	Sony CH 1400 CE
Video recorder	Sony SC-F1E
Colour printer	HP Paintjet

Software

Much effort and man power has been spent on software development for controlling the SMAL system, collecting the data, processing, analysis and measuring. This is a continuing effort which will not be further discussed.

3 SOME TYPICAL EXAMPLES

In this chapter some typical results obtained with the SMAL lidar will be shown. The data presented here were recorded with a repetition rate between 3 and 10 Hz and analogue pre-processed with a logarithmic amplifier. The pre-processed data were range compensated to correct for the geometric attenuation. Finally the results were converted to a false colour or gray scale representation in which the backscatter value is colour-coded and time and range are plotted along the axes. In this way an overview of the whole data record can be provided. At this moment 16 different colours or gray values are available for presentation on the computer screen. The sequence of colours has been chosen such that they correspond with the optical spectrum. In most figures the colour scale is visible in the right. Because the number of colours is limited, only part of the information can be presented in one figure. Either the fine structure is visible in a small interval of the signal amplitude (smaller and larger data values not visualized) or the whole signal amplitude interval is visible with the fine structure not resolved (fine structure data falls within one colour). The choice for a representation depends on the purpose of the plot and is made ad hoc by the operator. In the next few pages some results are presented.

Different measurement methods are distinguished:

1. measurements in a fixed direction
   a. horizontally
   b. under a positive elevation angle
   c. vertically
2. vertical scans or RHI (range to height indicator)
3. horizontal scans or PPI (plane position indicator)

Furthermore combinations of these patterns are possible. For each category at least one example will be presented. With the SMAL system conical scans are also possible.

1. Measurements in a fixed direction

Figure 3.1 shows an example of scattering from smoke patches in a time versus range plot when the system was pointed (almost) horizontally in a fixed direction over a smoke source. The wind was towards the lidar. The patches of smoke drifting in the direction of the lidar are visible. The sample frequency was 3 Hz and the range to the smoke source was 270 m. The figure shows a sequence of 500 measurements.

An other example of a horizontal measurement is shown in Figure 3.2. Here the lidar operated in a clear atmosphere parallel with the wind and at a small elevation angle. The repetition rate was 10 Hz and the maximum range was 1.5 km. The structure of aerosol cells or eddies, observed with the lidar, are not visible by eye. It is clear that the eddies now move away from the lidar. This figure is a typical example where only the small modulation of the lidar signal has been visualized.

Other figures with aerosol eddies driven by the wind are presented in Chapter 4.

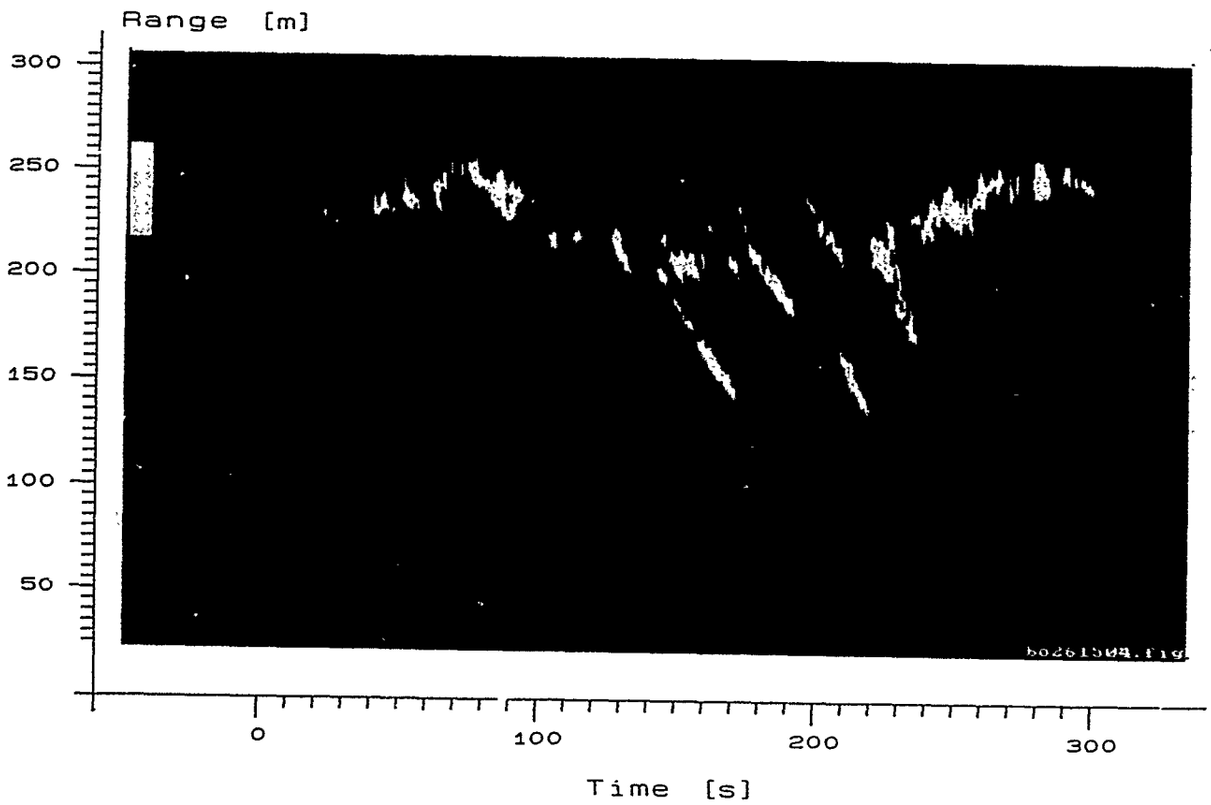

Fig. 3.1: A sequence of 500 backscatter profiles as measured with lidar and coded in false colour in a range (vertical axis) versus time (horizontal axis) plot. The sample frequency was 3 Hz in a fixed direction, over a smoke source. Patches of smoke drifting with the wind in the direction of the lidar are visible.

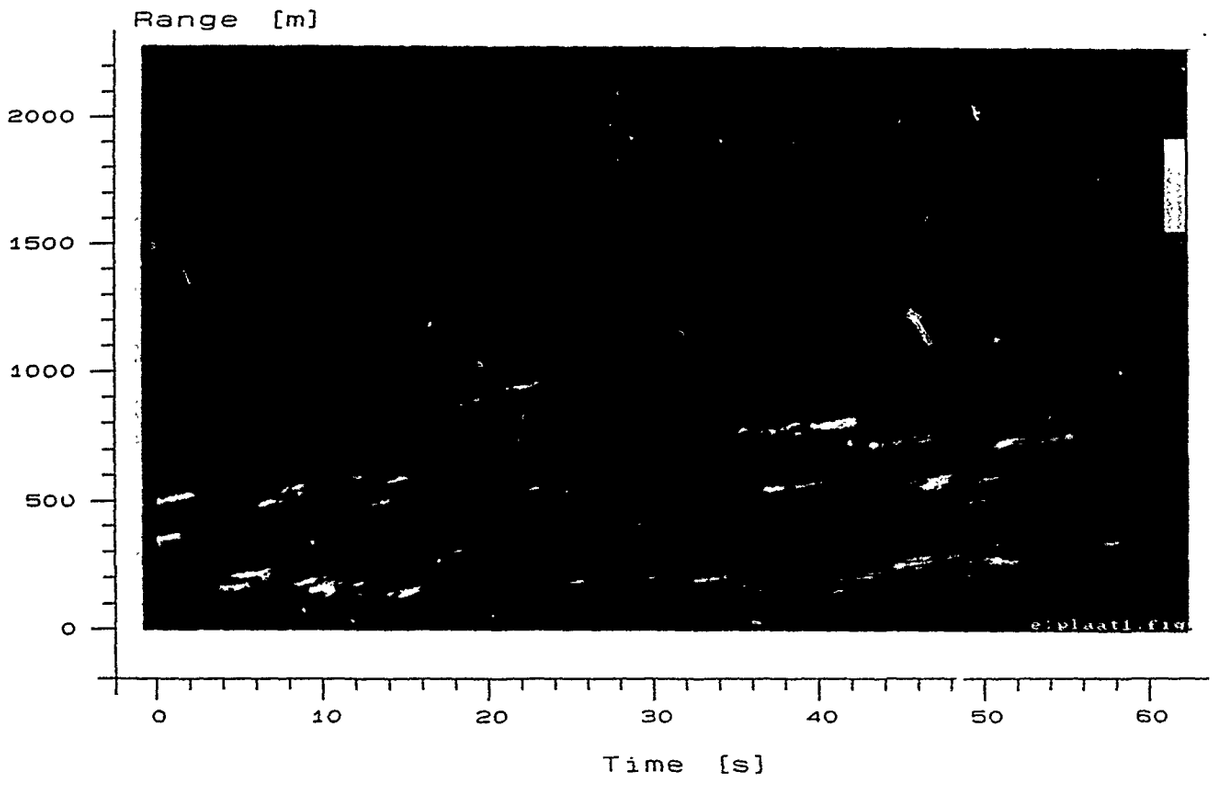

Fig. 3.2: Atmospheric scattering as measured with lidar and coded in false colour, in a time (horizontal axis, 0-60 seconds) versus range plot (vertical axis, 0-2280 m). The aerosol eddies are drifted by the wind, away from the system.

The next three examples show the results of measurements in the vertical direction. Figure 3.3 shows an example of a rather turbulent mixed layer and a more quiet atmosphere at higher altitudes. The maximum altitude recorded was 3 km and the recording time was 1 minute.

Figure 3.4 shows a quiet well-mixed layer with a depth of about 500 m. Above the mixed layer the atmosphere is less turbid and horizontally stratified. Because the visibility was very good in this situation, the signal to noise ratio is low.

The last example in this series is shown in Figure 3.5. It shows the sharp edge of a cloud layer at about 2 km altitude and at lower altitudes a stable mixed layer with some structure in the lower level.

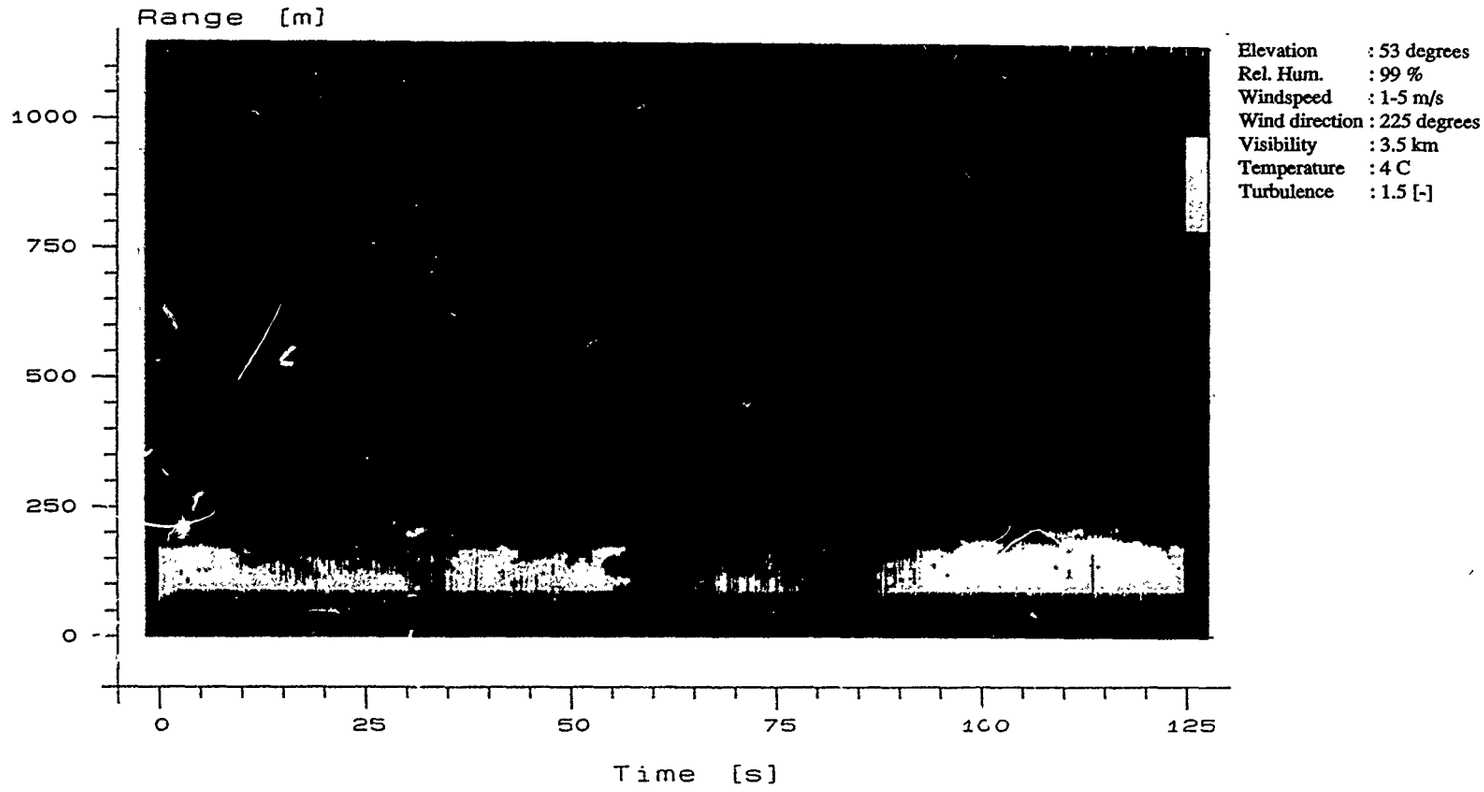

Fig. 3.3: Atmospheric scattering as measured with the lidar pointing vertically, showing the turbulent mixed layer at low altitudes (about 200 m) and the quiet atmosphere above the mixed layer. (vertical axis 0-1140 m, horizontal axis 0-128 seconds)

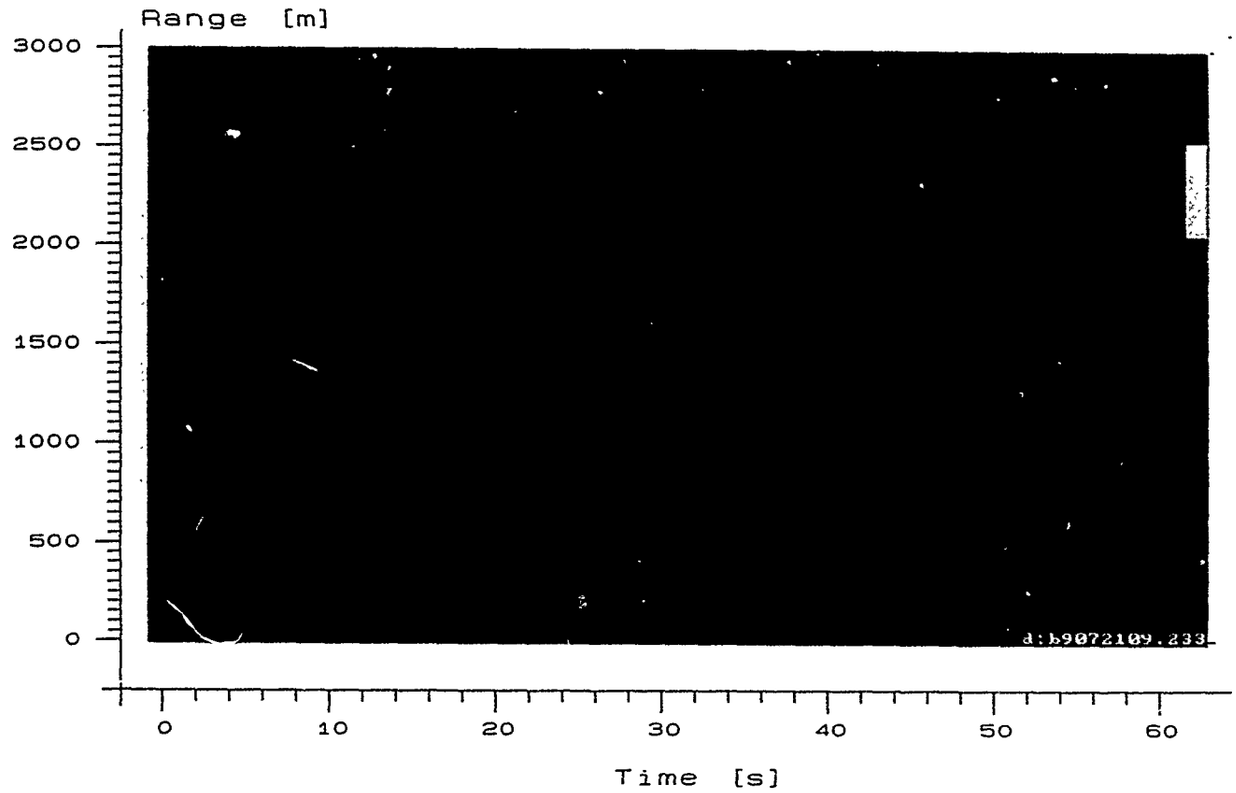

Elevation : 52 degrees
Temperature : -
Rel. Hum. : -
Windspeed : 2.5 m/s
Wind direction : 90 degrees
Visibility : 4.5 km
Pressure : 774 mm Hg
Cloud Cover : 8/8
(see also Figure 3.8)

Fig. 3.4: A smooth and convolving pattern of the atmospheric backscatter in the mixed layer as measured with the lidar pointing vertically. Above about 800 m altitude, a horizontal stratification is visible (horizontal axis: 0-60 seconds; vertical axis: 0-2850 m). See also Figure 3.8.

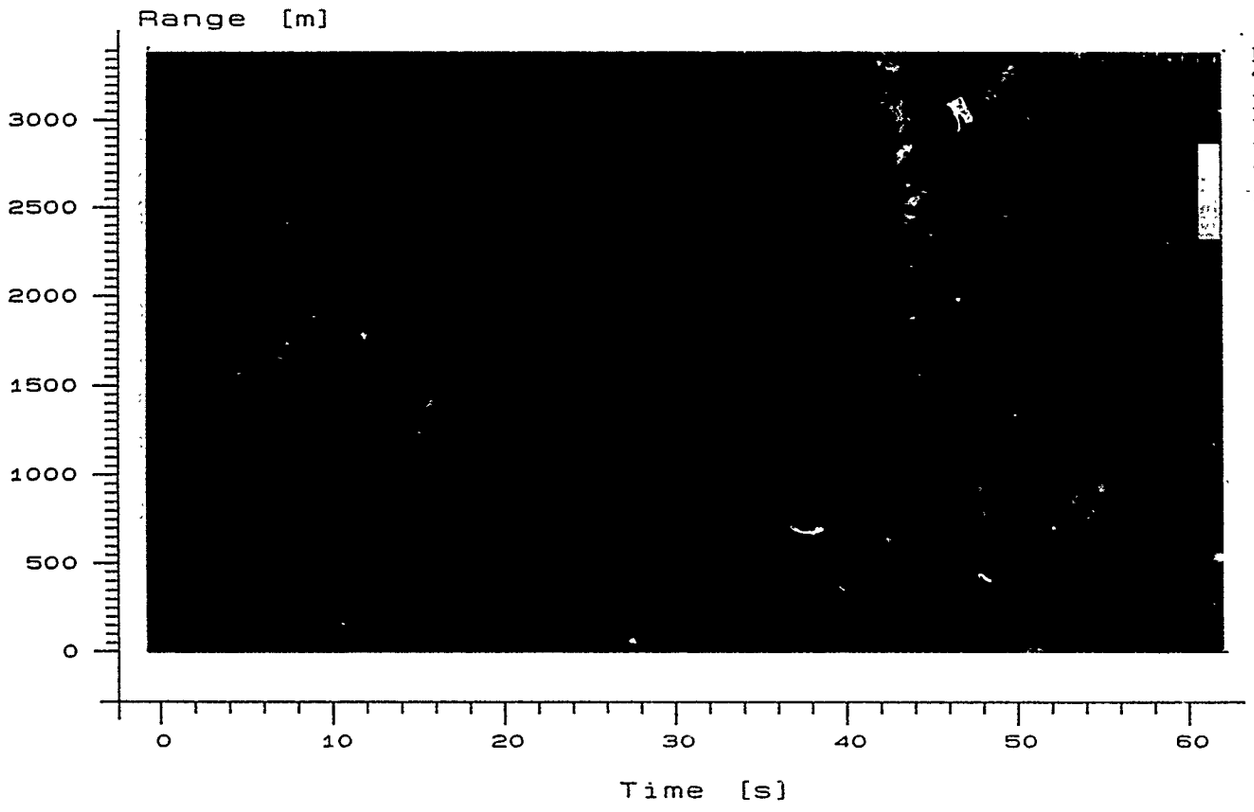

Fig. 3.5: Atmospheric backscatter profiles showing the sharp edge of a cloud layer and slight variations of the mixed layer at lower altitudes (horizontal axis: 0-60 seconds; vertical axis: 0-3420 m).

2. Measurements in a vertical plane

Figure 3.6. shows a vertical cross section of the atmospheric backscatter measured within a period of 15 seconds recorded over a range of 3 km. The cloud layer is clearly visible and also some scattering from above the cloud is observed. Furthermore the cloud eddies are visualized. This type of measurement can be used for locating smoke plumes and measuring their cross section.

Time series of such figures might give an insight in the dynamic behavior of the atmosphere. Two different examples are presented in the next two figures. Figure 3.7 has been recorded with a rather low angular resolution but the stratification of the atmosphere as well as the large dynamics in the scattering are well visible. Most remarkable is the detection of a second and a third cloud layer at larger altitudes (not visible by the human eye due to the strong radiation of the lowest layer).

Two sequentially recorded vertical cross sections of a clear atmosphere are presented in Figure 3.8. Here a large eddy is visible in the mixed-layer as well as a clear, horizontally stratified, layer at larger altitudes. The white stripes in the figure are caused by double pulses from the laser and are not atmospheric returns.

The last example of a vertical atmospheric cross section is shown in Figure 3.9. Although the number of samples is rather limited, some interesting features are visible. First a cloud layer is visible at about 1000 m altitude. At about 45 degrees from the horizon, part of this layer was not detected due to screening by a cloud patch at about 400 m. No signal at all is detected above the clouds (the structure above the cloud is only noise). Furthermore a local maximum in backscatter is visible below the higher cloud layer and finally the convolved top of the mixed layer can be distinguished. This last phenomenon has earlier been reported by Sasano, 1982 and has also be seen by radar, see e.g., Konrad, 1970 and Battan, 1973.

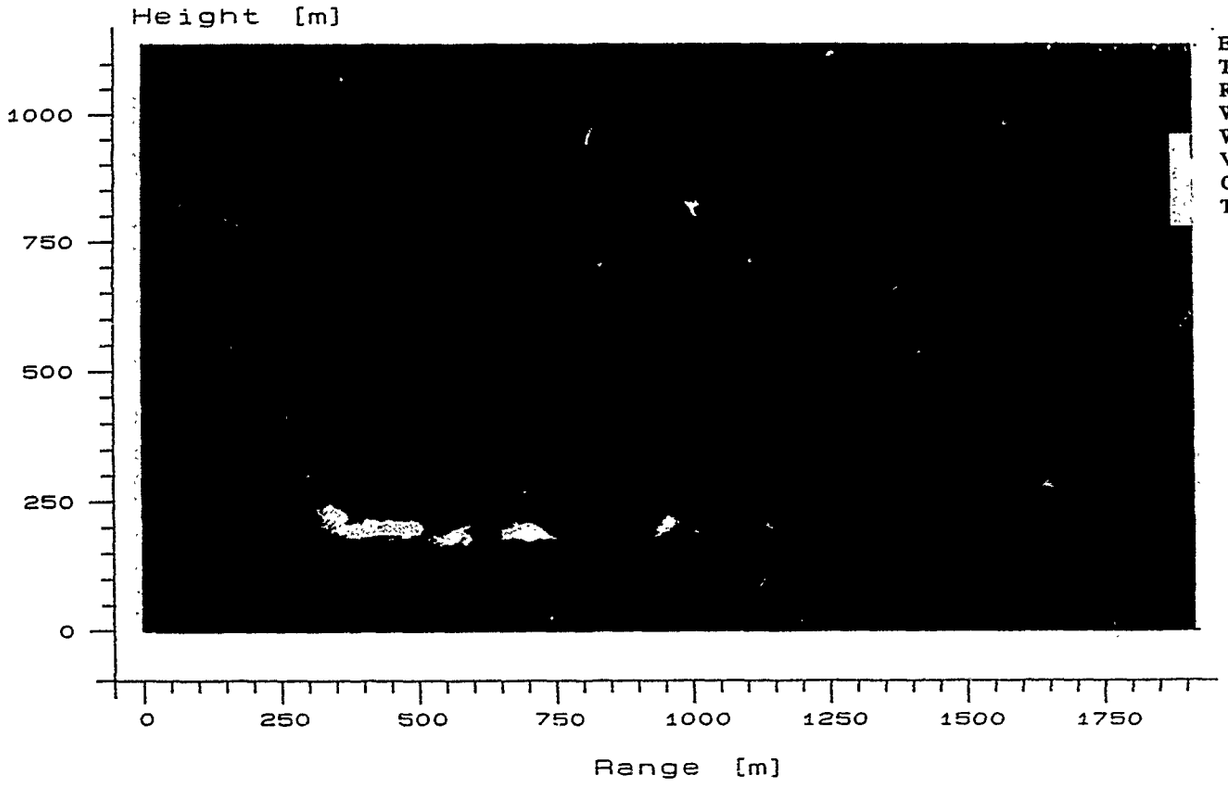

Fig. 3.6: A vertical cross section of atmospheric backscatter as measured with the lidar in a range to height indicator (RHI) scan. Scale: horizontal 0-1920 m and vertical 0-1140 m. Visible are the cloud altitude, spatial shapes of the cloud eddies and some backscatter from above the cloud layer.

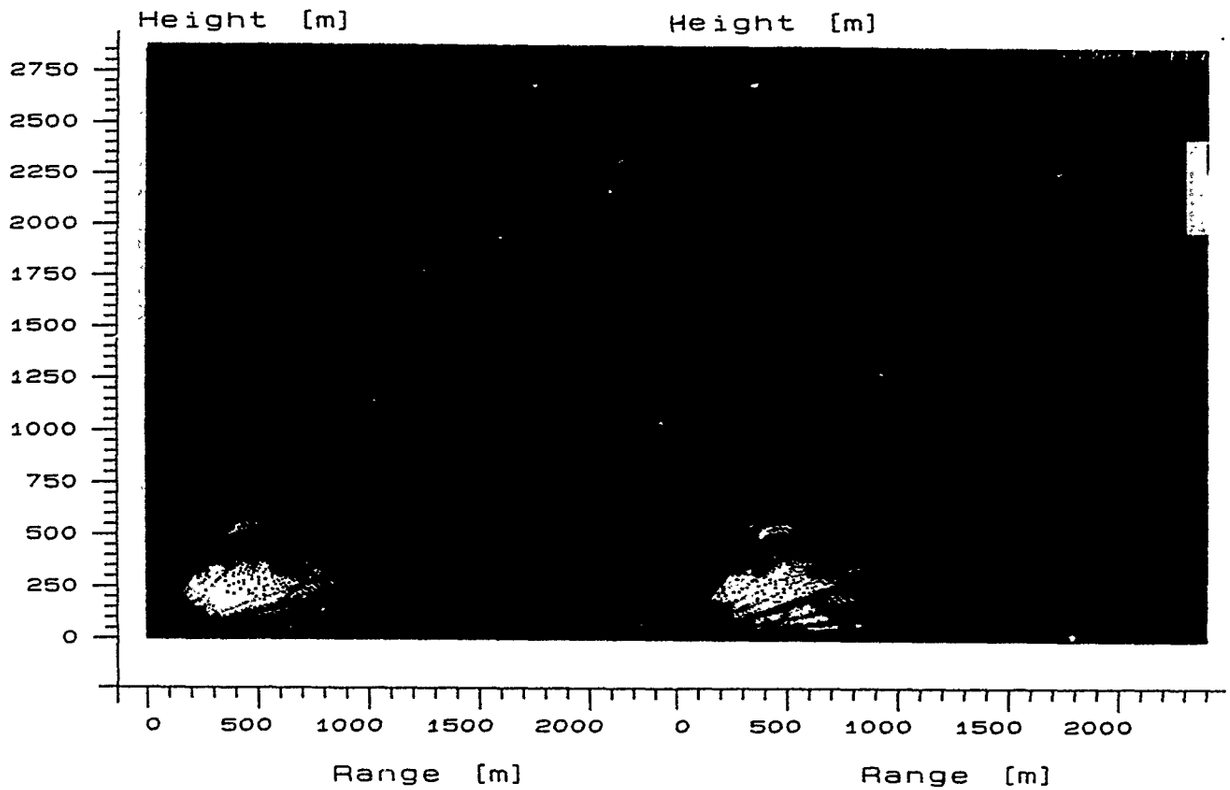

Elevation : 3..60 degrees

Fig. 3.7: Two sequentially measured (within 10 seconds) vertical cross sections of a turbulent atmospheric mixed layer. Three cloud layers are visible at xx, yy and zz. Scale: horizontal 0-2400 m and vertical 0-2850 m.

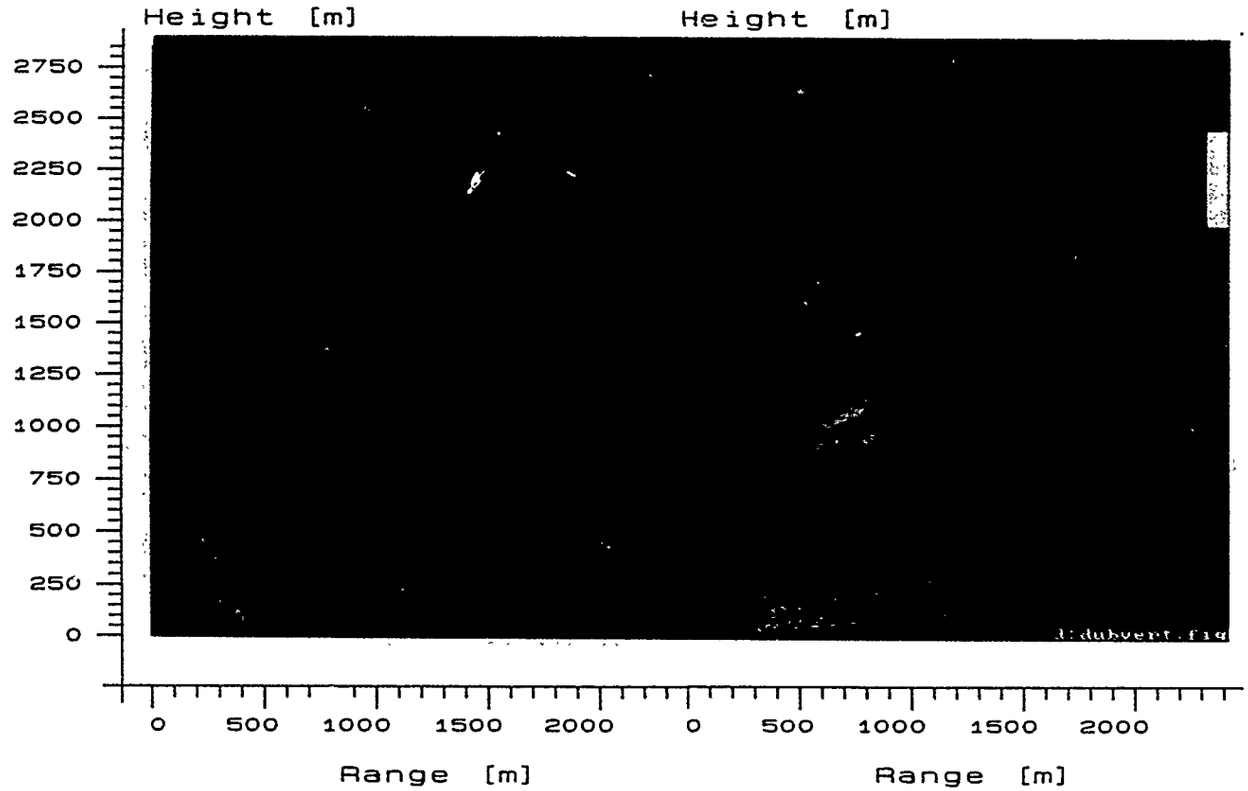

Elevation : 3..60 degrees
Temperature : -
Rel. Hum. : -
Windspeed : 2.5 m/s
Wind direction : 90 degrees
Visibility : 4.5 km
Cloud Cover : 8/8
Pressure : 774 mm Hg
(see also Figure 3.4)

Fig. 3.8: Vertical cross sections of a clear atmosphere measured within 10 seconds, showing the convolving mixed layer and a clear horizontal layer at higher altitudes. (see also Figure 3.4) Scale: horizontal 0-2400 m and vertical 0-2850 m.

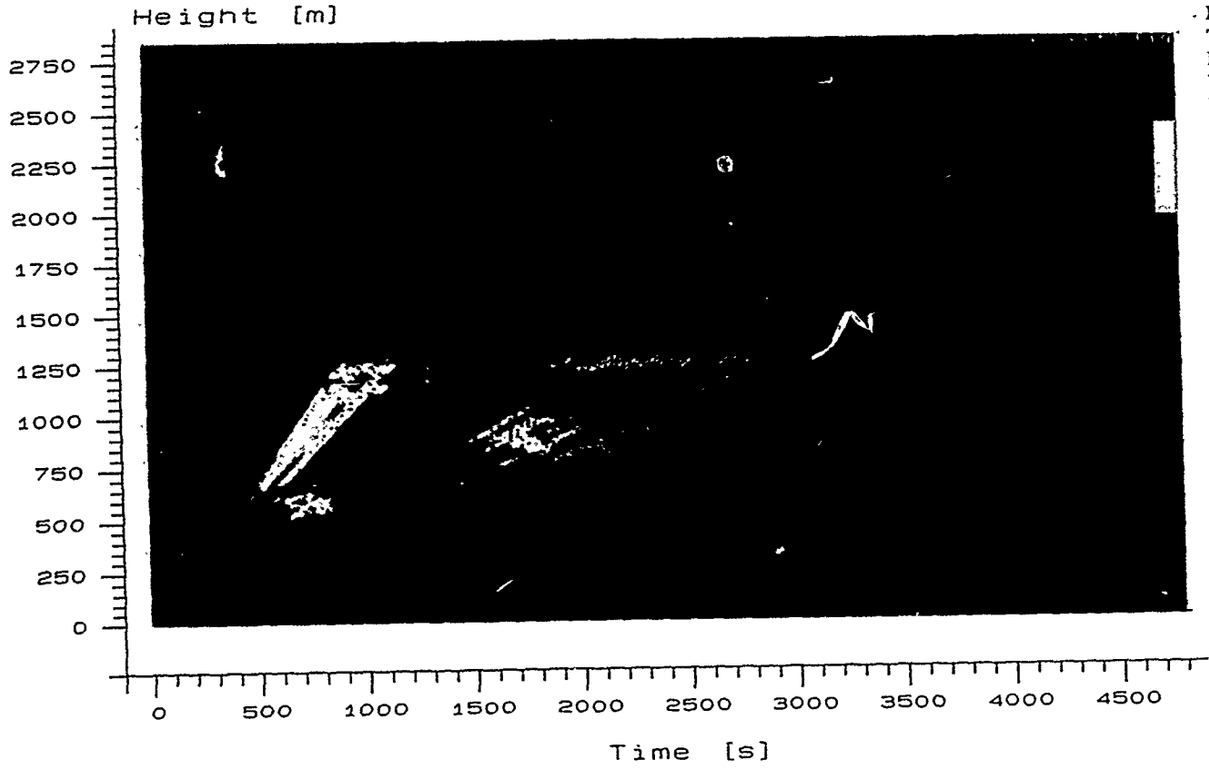

Fig. 3.9: Vertical cross section of the atmosphere as measured with the lidar and representing a convolved boundary layer with the backscatter increasing above about 500 m altitude, a small cloud layer at 700 m altitude obscures the high altitude cloud at about 1500 m. Scale: horizontal 0-4800 m and vertical 0-2850 m.

3. Measurements in a horizontal plane

Operating the lidar horizontally or at a small elevation angle with the platform rotating around the vertical axis, a horizontal or near horizontal cross section of the atmosphere is obtained. This method is useful for mapping plumes, turbulence structure etc. or for surveillance purposes. A typical example of a time series of horizontal cross sections of the atmosphere is presented in Figure 3.10. Here the size of a plume has been mapped at four different elevations and over an area of 240x143 m^2. The source of the plume is in middle of the left horizontal axis of each plot.

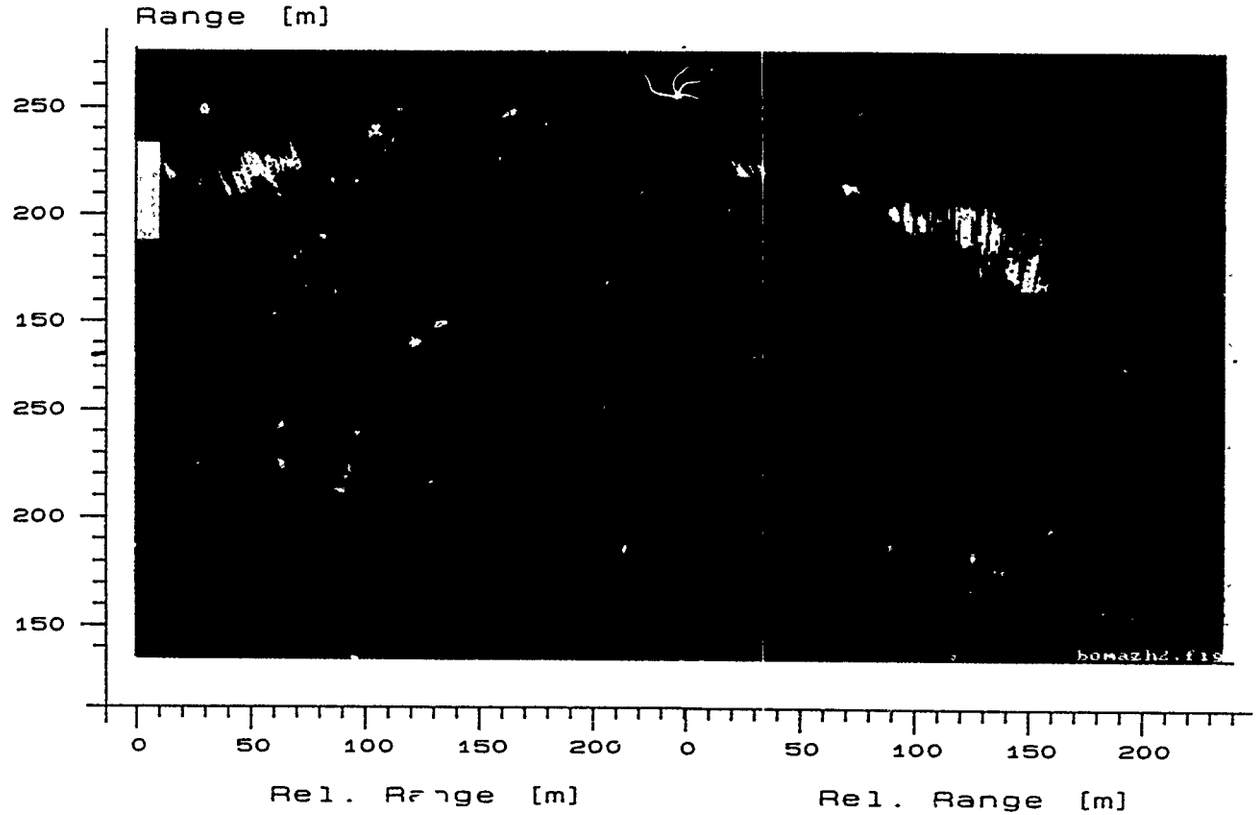

Fig. 3.10: Four horizontal cross sections (at different elevations) of a smoke cloud in the atmosphere over an area of 240x143 m^2

4 WIND MEASUREMENTS

4.1 Introduction

It has been shown in the previous chapter that aerosol eddies can be detected with a single channel laser radar (see, e.g., Figure 3.1). If it is assumed that these eddies have the same speed and direction as the wind, they can serve as a tracer for wind measurements. This idea is not new. Derr (1970) proposed a method to measure the wind vector with a lidar by measuring the transient time of aerosol eddies over a given path. Eloranta (1975) published results of wind speed measurements based on the principle of following the aerosol eddies with a Mie lidar over ranges to a maximum of 7 km. These measurements were further extended to three-point measurement by Stroga, 1980. Other articles on this principle were published by, e.g., Kunkel, 1980, Clemesha, 1981, Hooper, 1986 and Kolev, 1988. Wind measurements based on the analysis of lidar-measured PPI figures over a large area were published by, e.g. Sasano, 1982 and Ferdinandov, 1984.

4.2 Radial wind detection

By pointing the lidar parallel with the wind vector, as shown in Figure 4.1, the aerosol eddies moving towards or away from the lidar can be detected by a series of measurements in a fixed direction. An example of this kind of measurement is shown in Figure 4.2. The cross section of the cells as well as their speed can be determined from the figure. If the lidar is pointed perpendicular to the wind vector the aerosol eddies are illuminated normal to their direction of movement. The pattern shown in Figure 4.3 cannot unambiguously be related to wind speed because the sizes and the slopes of the individual eddied are unknown. Furthermore vertical airflow may influence the observed transient times of the eddies. (Figure 4.3 shows the results of such a measurement which was done some minutes before recording the previous figure.)

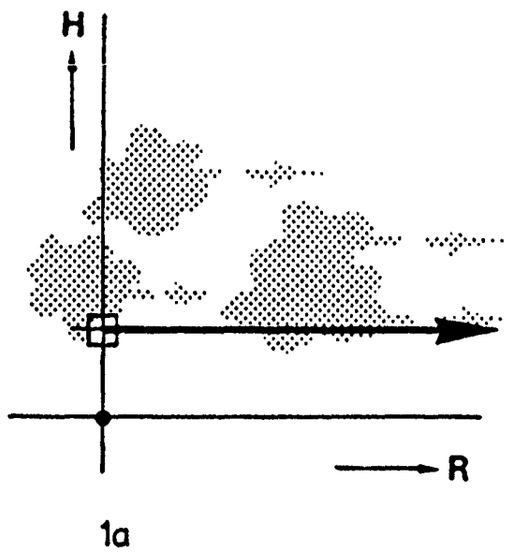

Fig. 4.1: Schematic representation of the lidar direction for radial wind speed measurements.

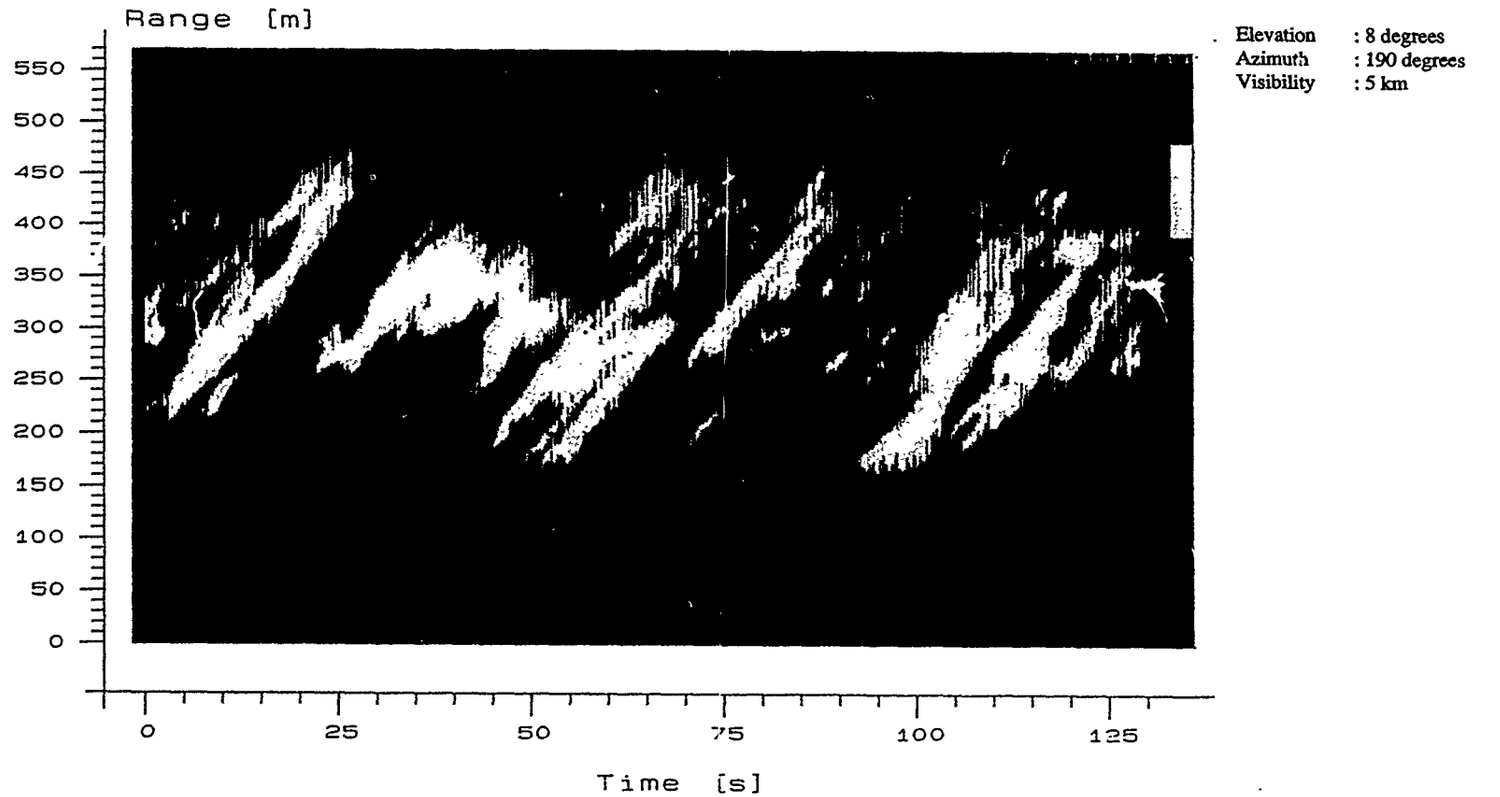

Fig. 4.2: Atmospheric backscatter, measured in the direction of the wind vector and coded in a false colour, in a range (vertical axis 0-570 m) versus time (horizontal axis 0-130 s) figure. Note that the eddies move away from the lidar and change in shape due to turbulent effects.

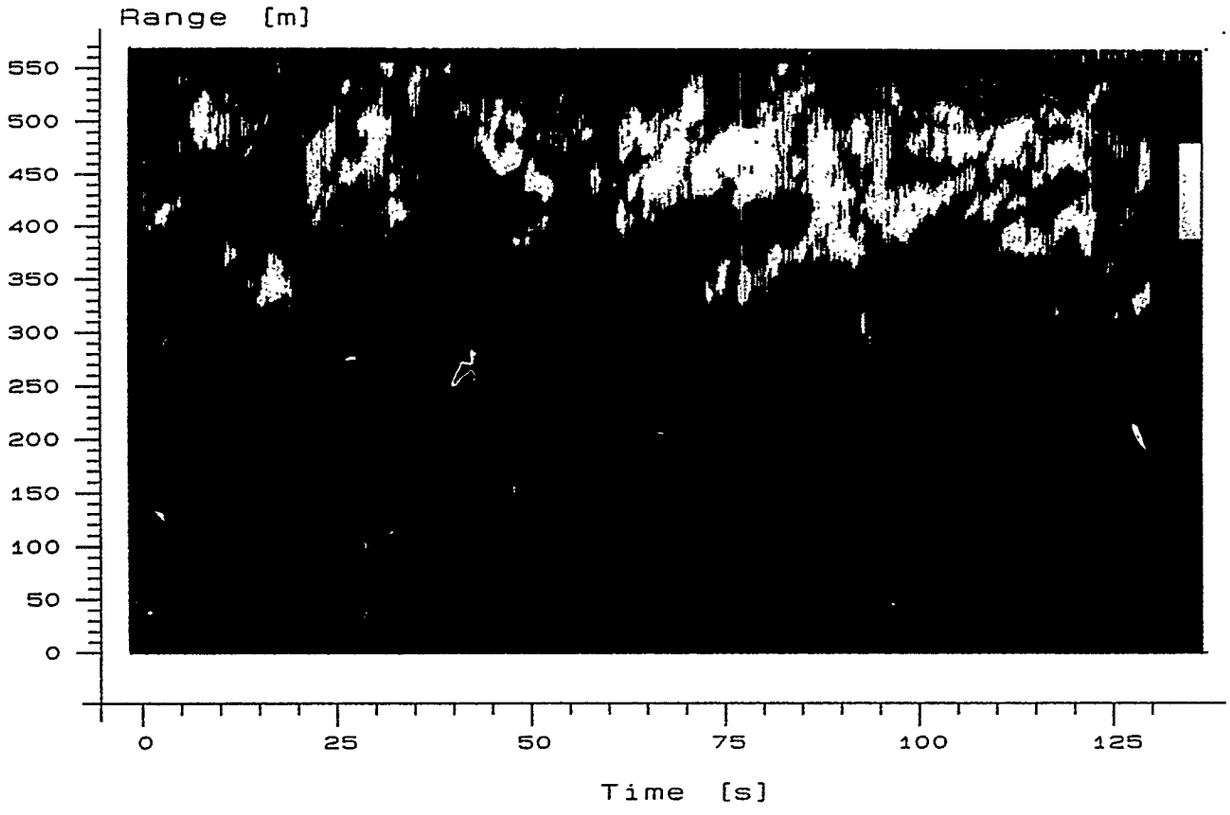

Fig. 4.3: Atmospheric backscattering, perpendicular to the wind vector and coded in false colour in a range (0-570) versus time (0-130 s) figure. Note that the eddies remain at similar distances and that their shapes change somewhat in time.

The figures show eddies of about 100 m and less. The best performance of wind speed measurements with this method is obtained when the lidar is pointed in a horizontal direction because measuring vertically provides only information on the presence of the aerosol cells and their heights. (Wind direction can than only be inverted if the cell dimensions are known a priori). Furthermore it is necessary that the variations in aerosol concentrations between the eddies can be detected with the lidar. Practice shows that this is not always the case.

With a dual beam system the measurements can be performed under two different, but small, elevation angles. This principle is shown in Figure 4.4.

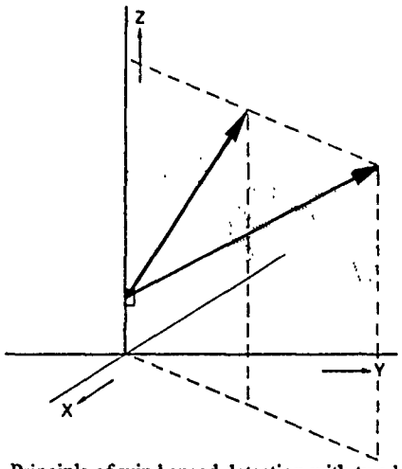

Fig. 4.4: Principle of wind speed detection with two beams. Correlation of signals at the same height can provide the wind speed.

By correlating signals from the same height, the time shift in combination with the geometry of the lidar provides a way to invert the wind speed (Hooper, 1986). The wind direction can be determined by performing a set of these measurements in different horizontal directions.

4.3 Cross wind detection

The wind speed perpendicular to the lidar axis can be determined with a dual beam system, shown in Figure 4.5. A two dimensional correlation is required to invert the wind speed from the two sets of lidar data.

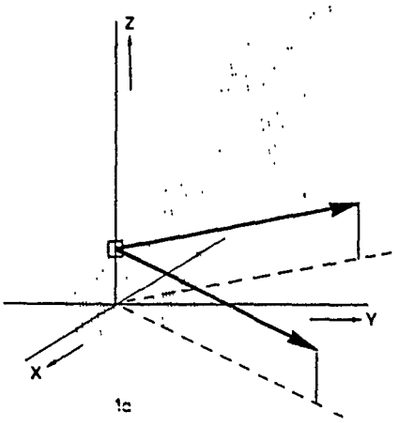

Fig. 4.5: Principle of a cross wind measurement with a dual lidar system. The windvector can be inverted by correlating the signals from the two lidars.

4.4 Wind measurements with a scanning lidar

With a scanning lidar there are more possibilities to measure the wind vector. For instance, the data obtained from a number of PPI measurements can be correlated. (However, a system with sufficient repetition rate is required.) The principle is the same as applied for cloud speed determination from satellite pictures, e.g., Leese, 1971.

The wind speed as a function of altitude can be determined by scanning the lidar in a vertical plane parallel to the mean wind speed. Here also the whole RHI figures must be correlated. If the wind direction is not known, measurements in different azimuth directions can provide this information. It should be noted, however, that the amount of data and the number of calculations will increase explosively. Furthermore the shape of the aerosol cells will change as they propagate with the wind, which reduces the accuracy of the result. An example of four consecutive vertical cross sections is presented in Figure 4.6 where some of the distinguished aerosol eddies, which drift with the wind, are indicated.

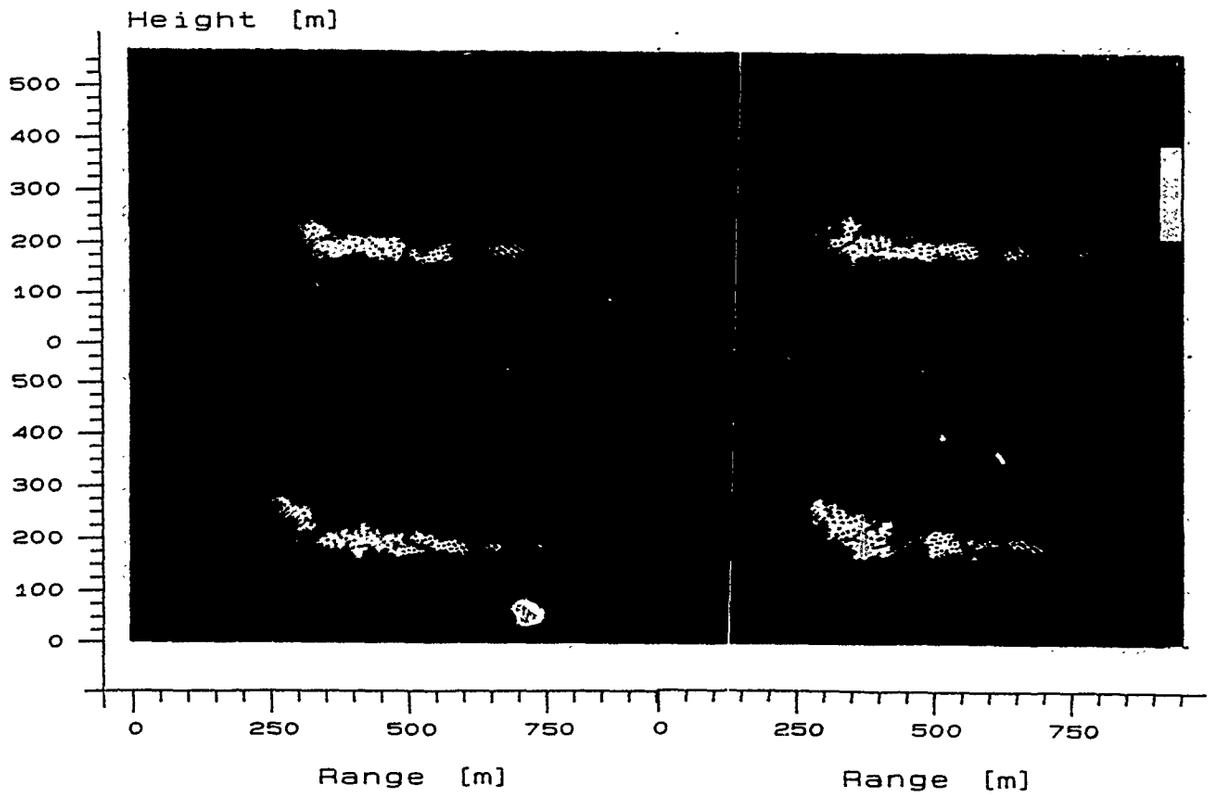

Fig. 4.6: Four consecutive, vertical cross sections of the clear atmosphere measured in the direction of the wind. Scale: horizontal 0-960 m and vertical 0-570 m. Some aerosol eddies (indicated) can be distinguished and drift with the wind.

Finally, a scanning lidar can also be used for application of the well known three point method for wind measurements. This principle is based on measuring the variation of atmospheric backscatter in three different directions around a given axis. By correlating the signals, the inversion of the wind vector should be possible. This has been published earlier by Clemesha, 1981. See also section 4.1.

4.5 Conclusion

Measurements of the wind vector are based on detection of aerosol concentration differences which are advected by the wind with the same speed. Measurements on a routine base have shown however, that these differences are not always present. It should also be kept in mind that the aerosol eddies change both in time and space which necessitates that the measurements are performed within a limited time.

5 CONCLUSION

Measurements by the Physics and Electronics Laboratory TNO with lidar systems thus far, provided information on the atmosphere with a time separation of 10 seconds to 6 minutes. These systems are well suited to investigate variations on a time scale of minutes to hours. The maximum range of these systems varied between 1 and 10 km. For studies on shorter time scales, lidar systems with a higher repetition rate are required. Such systems are already in use by other investigators (Eloranta, Sasano, Werner, Flament). With these high repetition rate systems the dimension time becomes better accessible to the user. Stack plumes can be measured in a shorter time interval, the dynamics of plumes, clouds and the clear atmosphere can be better visualized.

A lidar with a relatively high repetition rate (13 Hz) has been developed and constructed at the Physics and Electronics Laboratory TNO, which can measure in the clear atmosphere at ranges up to about 3 km. (Hard targets and clouds can be detected at much larger ranges). The system has been calibrated to perform quantitative measurements of the atmospheric backscatter. A rotating platform offers the possibility to point the system in every desired direction. The system is computer controlled. A second lidar has been mounted on top of the main lidar (unique design) for simultaneous measurements in different directions to investigate the feasibility of wind measurements.

To present the large amount of data (about 1 Mbyte/min) with this lidar, the method of false colour or a gray scale coding has been chosen for quick look and for presentation purposes. For quantitative results the data is stored.

The system is also suitable for testing alternative inversion methods for the vertical extinction profile as shown by Kunz, 1988.

The research efforts will be continued to measure the cross wind with the SMAL system.

ACKNOWLEDGEMENTS

The realization of a lidar system as described in this report is only possible in a cooperation with a group of people. Although all contributions are important, we can only mention here the largest ones. The complete lidar system, including the laser, has been constructed in the workshop of the Physics and Electronics Laboratory. First of all we are grateful to Hans Remmerswaal and Koos van der Ende for the mechanical work. Furthermore all the electronics, e.g., the amplifiers for the optical receivers, the controlling systems for the laser and the platform, were designed and constructed by Leo Cohen and Marcel Moerman. The software was initially written by Erik Nijboer. Thanks also to René Doeswijk for the excellent design of the revised version of the laser head. Last but not least, Kees Lamberts was the stimulating engine behind the screens, for large part of the project.

REFERENCES

Battan, L.J.,
Radar observation of the atmosphere
The University of Chicago Press, 1973
ISBN 0-226-03919-6

Clemesha, B.R.,
Remote measurement of the tropospheric and stratospheric winds by ground based lidar
Appl. Opt., Vol.20, No.17, 1 Sept. 1981

De Leeuw, G.,
Survey of aerosol and lidar measurements at the North Atlantic (25 May-28 June, 1983).
Physics Laboratory TNO, The Hague
Rep. PHL 1984-01

De Leeuw, G., in:
W.A. Oost a.o. HEXOS pilot experiment Meetpost Noordwijk, November 1984.
Filed project report: - chapter 7, Physics Laboratory TNO, The Hague

De Leeuw, G.,
Horizontal and vertical lidar measurements.
3rd Topical meeting on coherent laser radar, July 7-11, 1985, Gt. Malvern, UK

De Leeuw, G.,
Lidar measurements in the marine atmosphere.
International Conference on optical and millimeter wave propagation and scattering in the atmosphere, May 27-30, 1986, Florence, Italy

De Leeuw, G.,
HEXOS pilot experiment at Meetpost Noordwijk, November 1984: lidar and aerosol measurements.
Physics Laboratory TNO, The Hague
Rep. PHL 1986-17

De Leeuw, G.,
Modeling of extinction and backscatter profiles in the marine mixed-layer.
Appl. Opt. Vol. 28, 1989

Derr, V.E.,
A comparison of remote sensing of clear atmosphere by optical, radio and acoustic radar technique
Appl. Opt., Vol.9, No.9, Sept. 1970

Eloranta, E.W.,
The determination of wind speeds in the boundary layer by monostatic lidar
J. of Appl Meteor., Vol. 14, December 1975

Ferdinandov, E.S.,
Method of laser sounding of atmospheric dynamics
Bulg. J. Physics, Vol 11, 1984

Kolev, I.,
Lidar determination of winds by aerosol inhomogeneities; motion velocity in the planetary boundary layer
Appl. Opt., Vol. 27, No.12, 15 June 1988

Konrad, T.G.,
The dynamics of the convective process in clear air as seen by radar
J. Atmosp. Sci, Vol. 27, November 1970

Kunkel, K.E.,
Remote determination of winds, turbulence spectra and energy dissipation in the boundary layer from lidar measurements
J. Appl. Sci., Vol.37, May 1980

Kunz, G.J.,
Rotatie Raman Lidar
Physisch Laboratorium TNO, Den Haag
Report PhL 1978-07

Kunz, G.J.,
Lidar measurements during Oldebroek II
Physics Laboratory TNO, The Hague
Report PhL 1982-56

Kunz, G.J.,
Vertical atmospheric profiles measured with lidar
Physics Laboratory TNO, The Hague
Report PhL 1982-49

Kunz, G.J.,
Lidarmetingen bij de Amercentrale
Physisch Laboratorium TNO
Report PhL 1984-18

Kunz, G.J.,
Verslag van de Nederlandse bijdrage aan het European Vertical Structure Experiment,
Cardington, (UK), 16-29 january 1983
Physics Laboratory TNO, The Hague
Report PhL 1984-03

Kunz, G.J.,
A method for measuring the vertical extinction and backscatter profile with a scanning lidar
Physics and Electronics Laboratory TNO
Report FEL 1988-65, September 1988

Kunz, G.J.,
Digitaliseren van lidarsignalen al dan niet met een logarithmische versterker
Fysisch en Elektronisch Laboratorium TNO
Report FEL 90-I148, juni 1990

Lamberts, C.W.,
De experimentele laser radar
Physisch Laboratorium TNO, Den Haag
Report PhL 1974-40

Lamberts, C.W.,
Raman lidar; a feasibility study
Physics Laboratory TNO, The Hague
Report PhL 1975-49

Lamberts, C.W.,
Lidar; A statistical approach
Physics Laboratory TNO, The Hague
Report PhL 1978-31

Lamberts, C.W.,
Statistical analysis of the 1978 lidar measurements
Physics Laboratory TNO, The Hague
Report PhL 1980-41

Leese, J.A.,
An automated technique for obtaining cloud motion from geosynchronous satellite data using cross correlation
J. Appl. Meteor., Vol. 10, Febr. 1971

Sasano, Y.,
Convective cell structures revealed by Mie laser radar observations and image data processing
Appl. Opt., Vol. 21, No. 17, 1 Sept. 1982

Sasano, Y.,
Convective cell structures revealed by Mie laser radar observations and image data processing
J. Appl. Meteor., Vol.21, No.10, Oct. 1982

Stroga, J.T.,
Lidar measurement of wind velocity profiles in the boundary layer
J. Appl. Meteor. Vol.19, May 1980

Proceedings of the Workshop on Measuring and Modeling the Battlefield Environment
NATO report DS/A/DR(87)307
November 1987

UNCLASSIFIED

REPORT DOCUMENTATION PAGE (MOD-NL)

1. DEFENSE REPORT NUMBER (MOD-NL)	2. RECIPIENT'S ACCESSION NUMBER	3. PERFORMING ORGANIZATION REPORT NUMBER
TD90-4059		FEL-90-A352
4. PROJECT/TASK/WORK UNIT NO.	**5. CONTRACT NUMBER**	**6. REPORT DATE**
2136	A84KL122	APRIL 1991
7. NUMBER OF PAGES	**8. NUMBER OF REFERENCES**	**9. TYPE OF REPORT AND DATES COVERED**
42 (INCL. RDP, EXCL. DISTRIBUTION LIST)	30	FINAL REPORT

10. TITLE AND SUBTITLE
A HIGH REPETITION RATE LIDAR

11. AUTHOR(S)
G.J. KUNZ

12. PERFORMING ORGANIZATION NAME(S) AND ADDRESS(ES)
TNO PHYSICS AND ELECTRONICS LABORATORY, P.O. BOX 96864, 2509 JG THE HAGUE
OUDE WAALSDORPERWEG 63, THE HAGUE, THE NETHERLANDS

13. SPONSORING/MONITORING AGENCY NAME(S)
DMKL/OMAT

14. SUPPLEMENTARY NOTES

15. ABSTRACT (MAXIMUM 200 WORDS, 1044 POSITIONS)

USING OPTICAL RADAR (LIDAR) TECHNIQUES, PROPERTIES OF THE ATMOSPHERE CAN BE DETERMINED BY REMOTE SENSING. EXAMPLES ARE, E.G., THE HORIZONTAL VISIBILITY OR THE EXTINCTION COEFFICIENT, THE VERTICAL EXTINCTION OR VISIBILITY PROFILE AND THE CLOUD BASE ALTITUDE. BECAUSE THE TIME SCALES IN THE ATMOSPHERE ARE MUCH SHORTER THAN THE MAXIMUM SAMPLE RATE OF THE LIDAR AVAILABLE AT THE START OF THIS PROJECT, A NEED EXISTED OF A SYSTEM WITH A REPETITION RATE OF AT LEAST 10 PULSES PER SECOND. WITH SUCH A SYSTEM IT IS POSSIBLE TO MEASURE THE DYNAMICS OF THE ATMOSPHERE ON A SUB-SECOND TIME SCALE AND TO MAP SMOKE AND DUST CLOUDS. THIS REPORT DESCRIBES THE PROPERTIES OF SUCH A SYSTEM, DESIGNED AND DEVELOPED AT THE PHYSICS AND ELECTRONICS LABORATORY TNO. SOME TYPICAL EXAMPLES OF RESULTS OBTAINED WITH THIS SYSTEM ARE PRESENTED. THIS IS THE FINAL REPORT OF THE WORK PERFORMED UNDER ASSIGNMENT A84KL122.

16. DESCRIPTORS	IDENTIFIERS
LASER RADAR (LIDAR)	MIXED LAYERS
TMOSPHERIC PROPERTIES	VERTICAL ATMOSPHERE PROFILE
ID MEASUREMENTS	CLOUD MAPPER
CLOUD MEASUREMENTS	
EXTINCTION	
ATMOSPHERIC DYNAMICS	
MEASUREMENT ATMOSPHERIC COMPOSITION	

17a. SECURITY CLASSIFICATION (OF REPORT)	17b. SECURITY CLASSIFICATION (OF PAGE)	17c. SECURITY CLASSIFICATION (OF ABSTRACT)
UNCLASSIFIED	UNCLASSIFIED	UNCLASSIFIED

18. DISTRIBUTION/AVAILABILITY STATEMENT	17d. SECURITY CLASSIFICATION (OF TITLES)
UNLIMITED AVAILABILITY	UNCLASSIFIED